CROATICA CHEMICA ACTA
CCACAA **79** (2) 299–309 (2006)

ISSN-0011-1643
CCA-3094
Conference paper

Crystal Structure Dynamics: Evidence by Diffraction and Spectroscopy

Eugen Libowitzky

Institut für Mineralogie und Kristallographie, Universität Wien – Geozentrum, Althanstr. 14, A-1090 Wien, Austria
(E-mail: eugen.libowitzky@univie.ac.at)

RECEIVED DECEMBER 12, 2005; REVISED MARCH 7, 2006; ACCEPTED MARCH 10, 2006

Bragg diffraction is a major tool to solve and refine crystal structures, though it is limited as results obtained from the bulk sample are averaged in time and space. In contrast, spectroscopy is site sensitive, and thus a probe for local structure with high time and space resolution. Combination of both methods may reveal important additional information on crystal structures such as disorder and dynamics, and may even help avoid pitfalls in structure solution. Among the given examples are three minerals, *i.e.,* lawsonite, hemimorphite, leonite, which show phase transitions from dynamically disordered to ordered structures. Continuous evolution from order to dynamic disorder, however without a phase transition, is found in washing soda. Finally, examples of proton dynamics in a tetragonal garnet and in minerals with very strong hydrogen bonds are presented.

Keywords
hydrogen bonding
disorder
phase transition
infrared
water
hydroxyl

INTRODUCTION

Since the first days of X-ray diffraction, crystal structures have been solved and refined using the positions and intensities of Bragg reflections from single-crystal and powder diffraction experiments. Later on, the use of »light« sources different from X-rays, *i.e.*, neutrons, electrons, extended the use of diffraction experiments to crystals with very light elements, *e.g.,* hydrogen-bearing samples, and micro-samples in an electron microscope. However, though the method can give the full image of a crystal structure, information is always based on the more or less strict periodicity (long range order) of the crystal lattice.[1] Thus, the data are averaged over the whole sample, both in space and time. Therefore, information on local disorder (space) and dynamics (time), and on defects at only trace concentrations may be limited. (The recent method of measuring diffuse X-ray scattering[2] in the »background« region between the Bragg peaks to address these problems is not considered here.)

On the other hand, spectroscopy, and in this paper vibrational spectroscopy such as infrared (IR) and Raman spectroscopy are employed, will never result in full description of a crystal structure. However, since it does not rely on crystalline periodicity, non-crystalline materials such as gases, liquids, melts, glasses and metamict samples can be investigated. Moreover, because it is site-specific (a number of spectroscopic methods are even element-sensitive), even defects at low concentrations in a host structure and short range order phenomena may be studied. Finally, the excellent time resolution facilitates resolving dynamic processes much better than diffraction.[3]

STRUCTURAL INFORMATION FROM SPECTROSCOPY

Using vibrational spectroscopy, quantitative data can be obtained that provide useful structural information in three ways. Since the band energy (frequency, wavenumber) of a vibrational band is dependent on the mass and bond strength of the vibrating unit, *e.g.,* an O–H group, the peak positions provide important data on

bond lengths, like in the case of hydrogen bonds (see below). Absorption (IR) and scattering experiments (Raman) with polarized radiation on oriented, optically anisotropic samples result in data on the spatial orientation of a vibrating unit in a crystal structure (see below). Finally, by calibration of band intensities in a number of different ways, even information on the amount of a certain molecular species (down to trace concentration levels) in a sample can be obtained (see below). Because IR spectroscopy is frequently used in the examples given below, these quantitative IR techniques are described briefly (however, they work in a similar way also for Raman spectroscopy).

In a basic IR absorption experiment, a beam of IR light (modulated in frequency by a monochromator or in modern spectrometers by an interferometer) with intensity I_0 is absorbed by a molecular vibration in the sample and the remaining transmitted intensity I is recorded by the detector. The basic quantity I/I_0 is the transmittance T (usually expressed in [100 %]). However, since it is in logarithmic relation with thickness d and absorber concentration c, a more convenient unit is absorbance $A = -\log T$. According to the Beer-Lambert law, $A = \varepsilon \cdot c \cdot d$, it is in linear relation to sample thickness and absorber concentration; ε is the molar absorption coefficient.[4]

Correlation diagrams to derive hydrogen bond lengths from O–H stretching vibrations have been developed since the 1950s both from theoretical calculations[5] and from empirical studies.[6–9] In general, hydrogen bonds can be classified according to their bond lengths, *i.e.,* d(O···O), d(H···O), d(O–H), into very strong (very short): d(O···O) < 2.50 Å, strong (short): 2.50 < d < 2.70 Å, and weak (long): d > 2.70 Å with a barely defined upper limit beyond 3 Å.[10] Figure 1 shows the positive, curved correlation between O–H stretching wavenumber and O···O / H···O hydrogen bond lengths. The principle of this correlation is that with increasing hydrogen bond strength (decreasing H bond length), the H bond acceptor attracts the proton and thus elongates and weakens the O–H bond (~ 0.98 Å without H bonding), which in turn results in decreased stretching frequency (wavenumber). Further effects that correlate with increasing H bond strength are increasing peak width, and increasing anharmonicity.[4,7,11–14] Besides Figure 1, it is important for the examples below to realize that stretching vibrations are observed at 3200–3700 cm^{-1} for weak H bonds, at 1600–3200 cm^{-1} for strong H bonds, and below 1600 cm^{-1} for very strong bonds.[10] Finally, it must be stressed that in addition to H bonding, the cationic environment has also a (minor) influence on the wavenumber of O–H stretching vibrations.[15]

The spatial orientation of an O–H vector (or any other vibrational direction) can be derived from measurements with polarized IR radiation along the principal optical directions (the main axes of the indicatrix ellipsoid) in optically anisotropic crystals[16] (it is therefore impossible in cubic crystals). According to Figure 2, the absorbance components along the principal axes A_x, A_y, A_z are in a simple cosine squared relation to the total magnitude of the absorbance (as if measured parallel to the absorber). Thus, by measurements with IR radiation polarized parallel to all three main directions, the angles and consequently the orientation of the absorber are obtained. Moreover, the sum of the three components results in total absorbance, which is the correct quantity to estimate the concentration of the absorber.

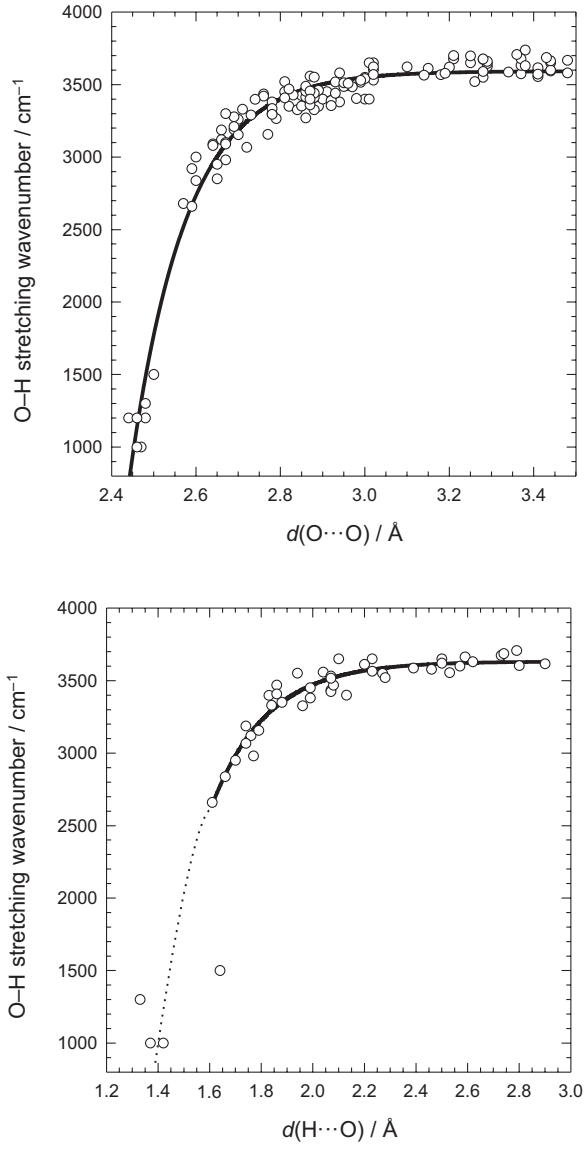

Figure 1. Correlation diagram between O···O / H···O hydrogen bond lengths and O–H stretching wavenumbers.[9]

Information about the concentration of a certain absorbing species is obtained by calibration of IR band intensities (preferably band areas are used instead of peak heights) with different analytical methods. In the case of hydrous species and defects in minerals, water contents

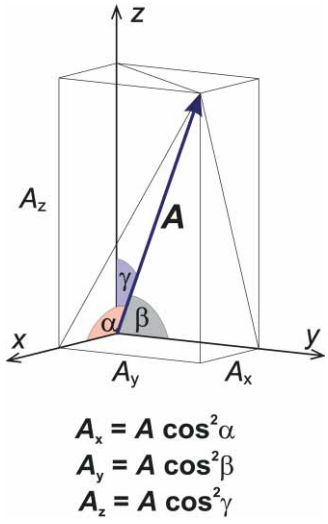

Figure 2. Sketch of an absorber with total absorbance A and components A_x, A_y, A_z that can be obtained by polarized IR absorption measurements parallel to main optical directions x, y, z.[16]

may be calibrated by heating the crushed (and milled) sample, and detection of the expelled water vapor by various methods.[17] Because of water adsorbed at grain surfaces, results are sometimes inaccurate. Bulk methods, *e.g.*, proton magic angle spinning nuclear magnetic resonance (^{1}H MAS NMR), nuclear reaction analysis (NRA), and secondary ion mass spectrometry (SIMS), avoid this disadvantage but are available only in rare, large-scale facilities. Finally, a general calibration using stoichiometric compounds was worked out, indicating a strong positive correlation of the molar absorption coefficient with the H bond strength.[18,19] Nevertheless, results of recent years (and disagreement with the general trend) confirm the necessity of individual mineral-specific calibrations.[17]

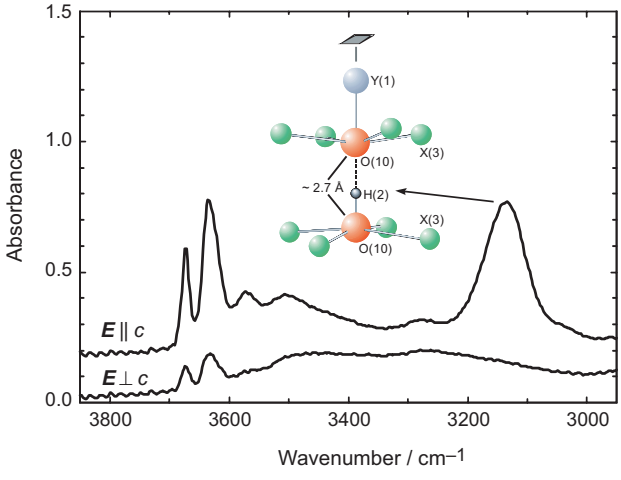

Figure 3. IR absorption spectra acquired with polarized radiation of vesuvianite from Rotkopf/Zillertal, Austria.[20] The inset shows a detail of its crystal structure around the strong hydrogen bond.[21]

A simple, illustrating example of the above mentioned structural constraints from IR data is given in Figure 3, showing spectra[20] acquired with polarized IR radiation of the tetragonal hydroxyl-bearing silicate mineral vesuvianite. The spectrum with the electric vector ***E*** of the polarized light parallel to *c* shows a band at ~ 3150 cm^{-1}, which is absent in the spectrum perpendicular to *c*. Thus, an OH$^-$ group with strong hydrogen bonding is expected (using Figure 1, an O···O distance of ~ 2.7 Å is derived) with orientation parallel to the *c* axis. This hydroxyl group (refined O···O H bond length ~ 2.70 Å) is actually observed by diffraction methods (inset in Figure 3).[21] In addition, weak or non-H bonded hydroxyl groups with various cationic environments and different orientations (~ 30° from the *c* axis) are confirmed by the bands at higher wavenumbers in both spectra. Using the band areas (integrated absorbances) and the general calibration trend of Libowitzky and Rossman,[19] a concentration ratio of 1 : 4 between the former and the latter hydroxyl groups is obtained (please note that the areas are not directly comparable!), which is in excellent agreement with the crystal structure refinement.[20,21]

LAWSONITE

Lawsonite, $CaAl_2Si_2O_7(OH)_2 \cdot H_2O$, space group *Cmcm*, is a hydrous high-pressure mineral. Due to its wide stability range, it is suggested to carry large quantities of water down to the Earth's mantle in subduction zones.[22] Its crystal structure consists of edge-sharing AlO_6 octahedra interconnected by di-silicate groups to a three-dimensional framework. The remaining interstitial cavities are filled with Ca atoms, H_2O molecules and OH$^-$ groups in highly symmetric positions (Figure 4).[23] Apparently, the latter two possess only weak (long) H bonds to neighboring oxygen atoms. The mineral shows a low-temperature phase transition at 273 K and another one at ~ 120–150 K. X-ray diffraction confirms that the framework of the structure is, in principle, preserved during all transitions, and structural changes affect most strongly only the hydrous species in the cavities. During the first transition, it appears from the single-crystal X-ray diffraction that the water molecule is rotated from its symmetric position at room temperature towards one of the hydrogen bond acceptors on the side (enhancing this H bond). In addition, the hydroxyl groups appear to be rotated to non-equivalent sites enhancing also one of the H bonds. Thus, this transition to space group *Pmcn* appears to be of a displacive type. During the second transition, the hydrous species deviate from their special positions in the drawing plane (Figure 4) and thus cause the non-centrosymmetric space group $P2_1cn$. Both reversible phase transitions can be nicely monitored by non-linear, partially abrupt changes in lattice parameters,

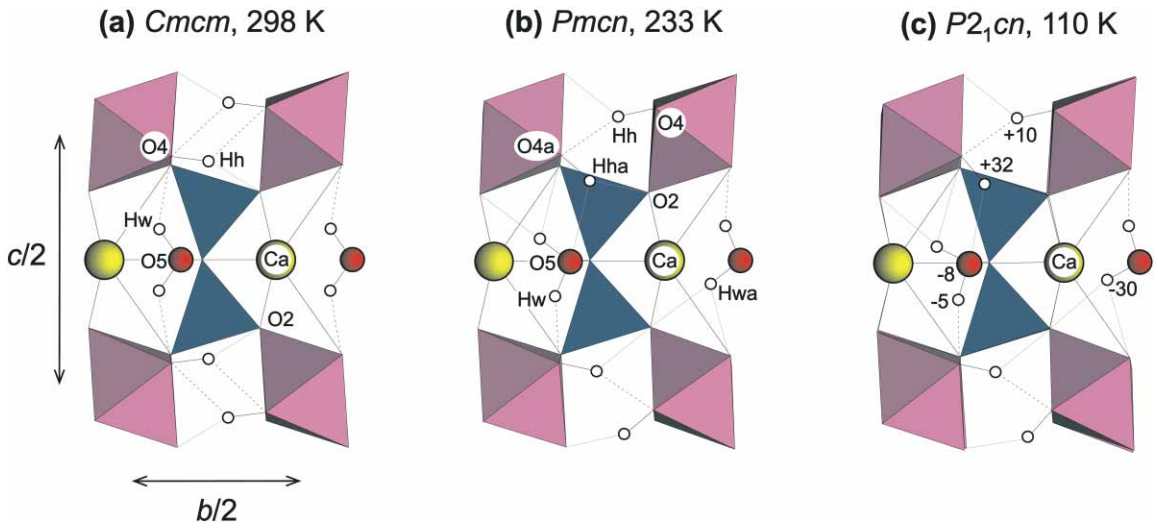

Figure 4. The crystal structure of lawsonite. (a) Room temperature structure with hydrous species in apparently highly symmetric positions. (b) Low-T structure with hydrous species »rotated« in the drawing plane. (c) Lowest-T structure with hydrous species deviating from the drawing plane (numbers denote deviations by 0.01 Å).[23]

X-ray reflection intensities, birefringence data, and H bond lengths with changing temperatures.[23]

IR spectroscopic investigations with polarized radiation of 3–4 μm thick, oriented and polished slabs of lawsonite[24] give quite a contrasting picture (Figure 5). The spectra evolve continuously (without abrupt changes) *versus* temperature. Two observations are of special interest: (i) There are strong peak shifts of the low-energetic modes with changing temperature. (ii) Nevertheless, even at room temperature two bands occur at low wavenumbers (Y: ~ 3200 cm^{-1}, Z: ~ 3000 cm^{-1}) and thus indicate strong hydrogen bonding. The former observation is the characteristic behavior of vibrational bands in the close vicinity of a displacive/order-disorder phase transition.[25] The latter fact, however, is in strong disagreement with the X-ray data at room temperature (only weak H bonding!) and thus requires revision of the crystal structure at room temperature and of the first phase transition.

A consistent picture of the room temperature structure of lawsonite is only obtained if the low time resolution of diffraction experiments is considered (see above). In the case of dynamic motions, this low time resolution may result only in diffuse centers of motion, whereas spectroscopy gives »snapshot«-like images of the endpoints of motion. Thus, the highly symmetric po-

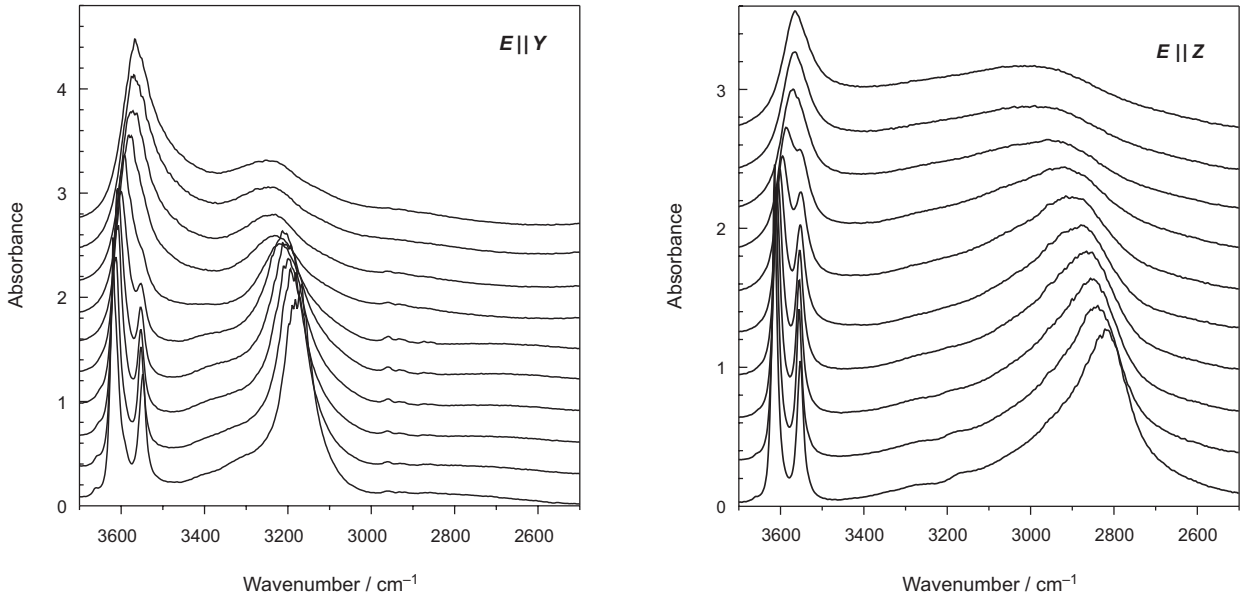

Figure 5. IR absorption spectra acquired with polarized radiation of lawsonite parallel to *Y* (left) and *Z* (right), at temperatures between 80 (bottom) and 325 K (top).[24] Note the strong and continuous shift of the low-wavenumber modes.

sition of the H_2O molecule in the center of the cavity of the lawsonite structure (as evidenced by X-ray diffraction) is only an average center of motion of the H_2O group. In reality, the H_2O molecule shows a rapid hopping motion between positions visible only in low-temperature diffraction experiments (where the hopping motion is frozen). This refined picture is then in agreement with the strong hydrogen bonds evidenced by spectroscopy at any temperature, and it is more reasonable from electrostatic considerations. An H_2O molecule in the center of a large cavity, attracted on both sides by H bond acceptors, would be as unstable as an iron sphere between the poles of two strong magnets.

The lawsonite hydroxyl groups show a similar dynamic behavior, hopping between positions visible in the low-temperature structures. This proton dynamics was also confirmed by neutron diffraction experiments, where the H atoms show large, elongated anisotropic displacement parameter (ADP) ellipsoids.[26] The short H bond distances at room temperature were confirmed also by proton NMR experiments (Gabuda & Kozlova).[27] The phase transitions are therefore not displacive but rather of a dynamic disorder-order type.

Recent investigations have shown that there are also small displacive variations in the framework of the structure (indicated by the strong peak shifts of the low-energetic IR absorption bands). Using optical, dielectric and elastic parameters, the thermodynamic character was shown by Landau theory to be tricritical in the first transition and second-order in the second transition. Pronounced precursor effects up to 200 K above the first transition temperature (well visible in birefringence data) may indicate fluctuations in the ordering scheme of the H bonds, *e.g.,* from short to medium range order, followed by long range order below the transition temperature. For these and further details see Sondergeld *et al.*[28] and references therein. Finally, it should be mentioned that these phase transitions were also observed in the isostructural, rare mineral hennomartinite, $SrMn_2^{3+}Si_2O_7(OH)_2 \cdot H_2O$.[29]

Summing up, it should be stressed that four important observations indicated the dynamic disorder-order phase transitions and led to the revised description of the crystal structure: (i) strong shift of IR bands with changing temperature; (ii) two H bond acceptors (energetic minima) in the close vicinity of the hydrous species, with the H_2O molecule apparently in an unstable position in-between; (iii) strongly anisotropic ADP ellipsoids (revealed by neutron diffraction); (iv) mismatch between diffraction and spectroscopy (H bond lengths in this case).

HEMIMORPHITE

The mineral hemimorphite, $Zn_4Si_2O_7(OH)_2 \cdot H_2O$, space group *Imm*2, is a common alteration product in the oxidation zone of zinc deposits. Its crystal structure shows four-membered rings of ZnO_4 tetrahedra interconnected by di-silicate groups to form a polar framework structure (Figure 6a).[30] The remaining channels are filled with hydroxyl groups and water molecules at apparently symmetric sites. The arrangement of the hydrous species along the channel axis is given in Figure 6b. These data from a neutron refinement[30] indicate strong dynamics of the H_2O and OH^- groups by the large and strongly anisotropic ADP ellipsoids. Moreover, there are two H bond acceptors for each hydroxyl group, *i.e.,* the oxygen atom of the water molecule and the oxygen atom of the opposite hydroxyl group.

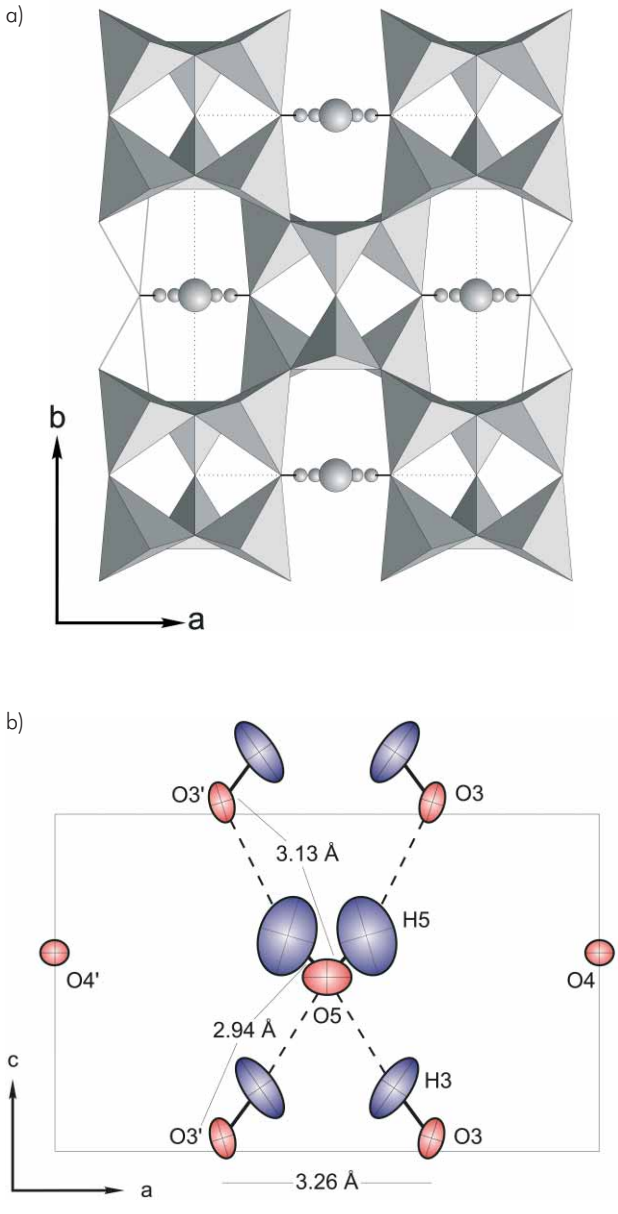

Figure 6. The structure of hemimorphite. (a) Projection parallel to [001]. (b) Projection parallel to [010] showing the content of the structural channels and indicating the strong dynamics of hydrous species by elongated ADP ellipsoids.[30]

Infrared spectra acquired with polarized radiation of 7 μm thin, oriented hemimorphite slabs[31] show two important features (Figure 7): (i) a strong shift of the O–H stretching vibration || *c* with changing temperature; moreover, this band at ~ 3400 cm^{-1} indicating a moderately strong H bond is in disagreement with any H bond distance of the structure refinement; (ii) three bands || *a* and one major band (besides weak maxima) || *c*, clearly visible at low temperatures. The former feature is a strong indicator of the vicinity of a phase transition (see above). The latter is in disagreement with vibrational modes calculated from a factor group analysis[32] of the hydrous species using the neutron data of Hill *et al.*[30] – Because of one symmetric (|| *c*) and one antisymmetric (|| *a*) stretching vibration of the two symmetric hydroxyl groups (vibrating in-phase and out-of-phase) and one symmetric (|| *c*) and one antisymmetric (|| *a*) stretching vibration of the water molecule, two bands are expected || *a* and two bands || *c*.

Thus all four indications of a dynamic disorder-order phase transition were observed (see above). The transition was finally confirmed by birefringence data at 98 K[31] and the low-temperature structure was refined with neutrons at 20 K.[33] This structure shows doubling of the *b* and *c* lattice parameters, resulting from the ordering of the hydrous species along the channel axis.

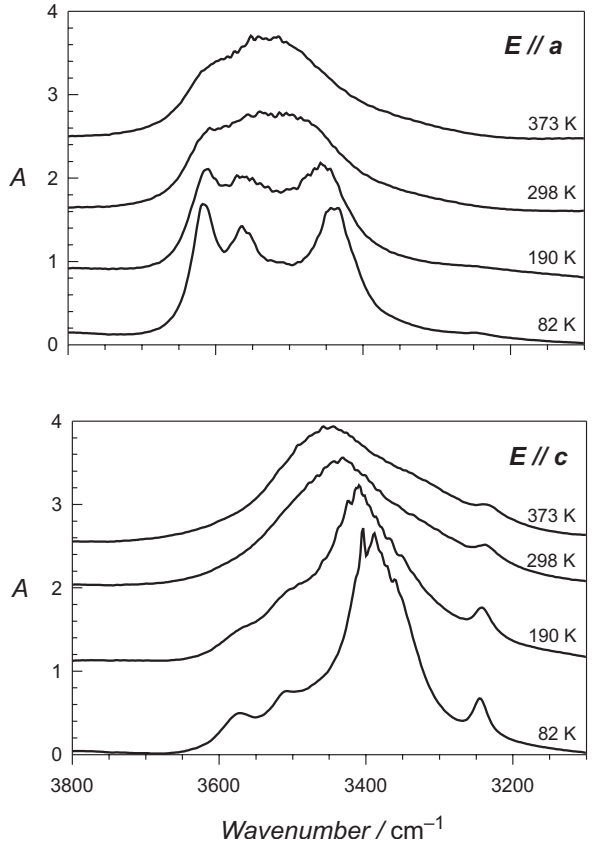

Figure 7. IR absorption spectra using polarized radiation of hemimorphite parallel to a (top) and c (bottom) at variable temperatures.[31]

The alternating rotation of the hydroxyl and water molecules leads to a continuous system of moderately strong H bonds and changed orientations of O–H vectors, which is in better agreement with the spectroscopic data. Similar to lawsonite, the apparently highly symmetric sites of the OH^- and H_2O groups in the room-temperature structure of hemimorphite[30] are due to the hopping motion between positions visible only in the low-temperature phase.

Dehydrated hemimorphite can be obtained by heating the mineral up to 500 °C for 12 hours. By this procedure, only the water molecules are expelled and the rest of the structure remains unchanged (similar to zeolite-like behavior). Single-crystal X-ray diffraction and IR spectroscopy with polarized radiation of oriented crystal slabs[34] still confirm strong dynamics of the hydroxyl groups; however, because of the missing water molecule (and thus the missing, most important H bond acceptor), no phase transition is observed down to 80 K.

LEONITE

Leonite, $K_2Mg(SO_4)_2 \cdot 4H_2O$, space group *C*2/*m*, occurs in the top layers of salt deposits and belongs to a group of isostructural minerals and compounds, of which the other members are synthetic »Mn-leonite«, $K_2Mn(SO_4)_2 \cdot 4H_2O$, and mereiterite, $K_2Fe(SO_4)_2 \cdot 4H_2O$. Its crystal structure (Figure 8) is basically composed of linear, corner-sharing units of SO_4-*Me*$(H_2O)_4O_2$-SO_4 units aligned parallel to the *a* axis in a distorted NaCl-like arrangement, interconnected by the K atoms and hydrogen bonds of the water molecules.[35] However, there are two different types (crystallographically different sites) of these linear units, one of them with dynamically disordered sulfate groups at room temperature, which is indicated by split, half-occupied oxygen atom positions (here simply indicated by A and B). In a schematic way of description, alternating layers parallel to (001) can be observed that contain either only disordered units (D) containing mixed A and B sites or only ordered units (O). Therefore, the sequence through these schematic layers along [001] is ...O D O D O D... (Figure 8). The disorder freezes at low temperatures and thus leads to reversible phase transitions.[35] The interesting point is that Mg- and Mn-endmembers show two low-temperature phase transitions, ordering at the first transition to space group *I*2/*a* with the sequence ... O A O B O A O B O A O B... As a consequence, the *c* lattice parameter is doubled. In the second, displacive transition at even lower temperatures, this ordered structure switches suddenly to another layer sequence ...O A O A O A... in space group $P2_1/a$ with approximately original lattice parameters. The Fe-endmember shows only one transition ordering at low temperature directly to the sequence ... O A O A O A... (Figure 8).[35]

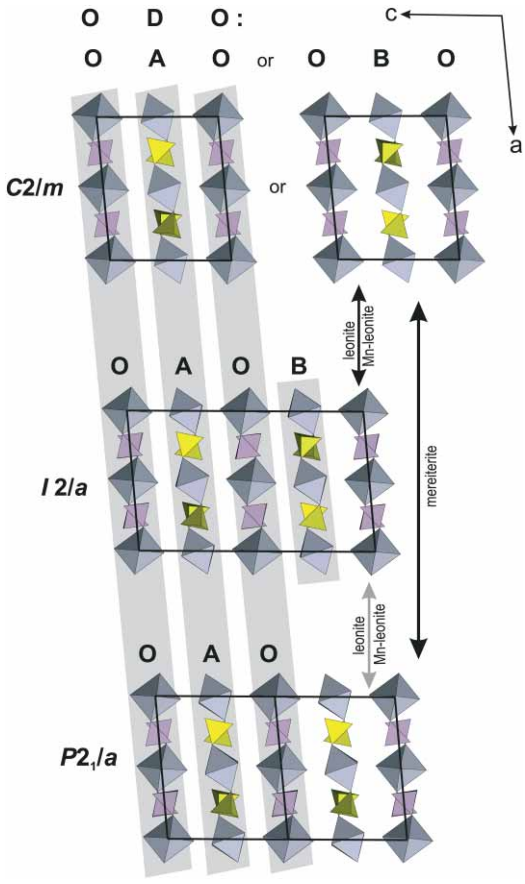

Figure 8. Crystal structures of leonite-type compounds and their changes from a disordered structure (ODO – top) to ordered structures (OAOB – center and OAO – bottom) at low temperatures.[35] Bold arrows indicate dynamic disorder-order transitions, the grey arrow indicates the sudden displacive transition of leonite and Mn-leonite.

In order to investigate the thermodynamic characters of these transitions, differential scanning calorimetry, optical, X-ray intensity,[36] and IR and Raman spectroscopic[37] measurements were performed at variable temperatures. In all cases, the first-order type of the second, displacive transition (at lowest temperatures) was confirmed by sharp discontinuities in the measured parameters *versus* temperature. The dynamic disorder– order transition, however, required a more detailed analysis according to Landau theory, which correlates certain measured, physical macroscopic quantities with the evolution of the order parameter (from 0 to 1) below the critical temperature of transition. Though data from all methods resulted more or less clearly in a tricritical character of the dynamic disorder to order transition, analysis of IR and Raman spectra showed very impressively the freezing of the dynamic behavior. Figure 9a depicts the evolution of Raman spectra in the region of sulfate vibrations across the transition temperatures. Whereas the first-order transition is visible by sudden band shifts, the ordering process is only indicated by a continuous change of band parameters. The nonlinearity of these changes is well discernible in Figure 9b.

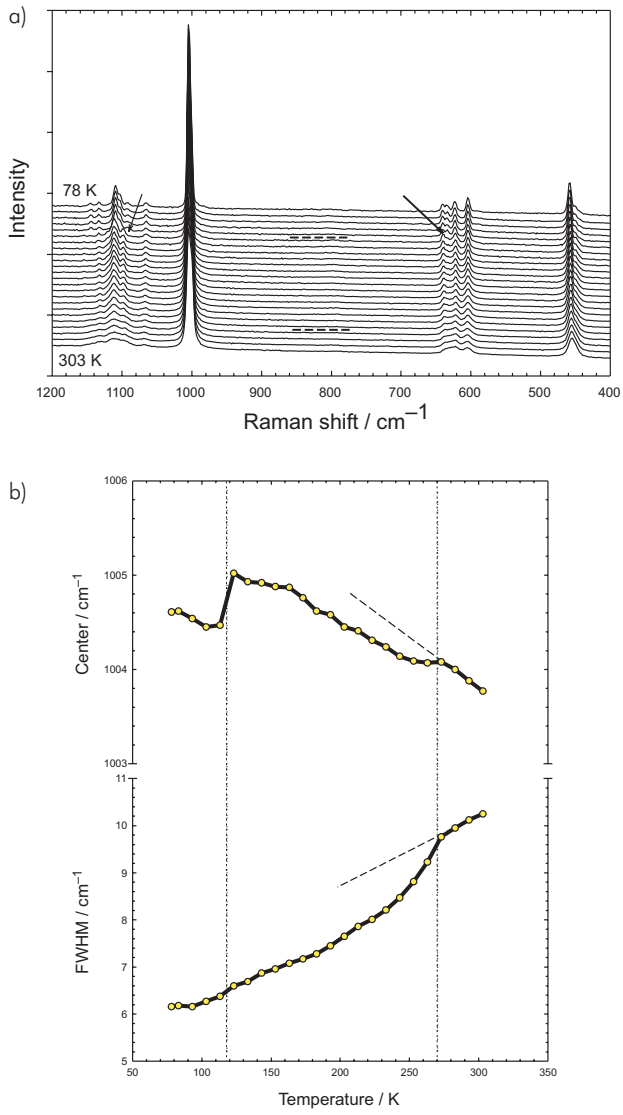

Figure 9. The evolution of Raman spectra of leonite with temperature. (a) The general appearance of the sulphate vibrational region.[37] Broken lines indicate transition temperatures, arrows point to sudden changes in the spectra. (b) The evolution of peak position and width (FWHM) of the sulphate stretching vibration *versus* temperature.[37] Dotted lines mark phase transition temperatures, broken lines indicate the extrapolated course of the data above the dynamic disorder-order phase transition.

The peak position of the symmetric stretching vibration is, of course, suddenly changed at the first-order transition due to an abruptly changed structural environment, whereas the ordering process is only barely indicated. In contrast, the peak width (FWHM) correlates nicely with the ordering process and indicates the dynamic disorder–order transition by a non-linearity in the data slope. Excess decrease of the FWHM data results in a critical parameter of ~ 0.25 in the evolution of the order parameter, thus confirming the tricritical character of the transition. The first-order transition at lower temperatures is not manifested by a change in peak width, as this sudden transition does not provide any change in the disorder and

dynamics of the structure (both low-temperature phases are ordered, only the ordering scheme is changed from OAOB to OA).

The different behavior of Fe- *versus* Mg- and Mn-endmembers is explained by the more distorted shape of the coordination polyhedron around Fe, which also acts on the whole hydrogen bonding scheme surrounding and connecting the structural units.[38] In general, these H bonds with O···O distances as short as ~ 2.65 Å are shortened, on the one hand, and elongated, on the other, during the ordering process at low temperatures (though the evolution of bond lengths is more complex in detail). This behavior is in good agreement with that of H bonds in lawsonite and hemimorphite described above.

WASHING SODA

The mineral natron, $Na_2CO_3 \cdot 10H_2O$, space group *Cc*, occurring as a rare mineral in nature, is an important synthetic compound used in detergents and thus commonly known as »washing soda«. Its crystal structure is composed of groups of edge-sharing hydrated sodium octahedra, $Na_2(H_2O)_{10}$, and carbonate groups. These units are in an NaCl-like arrangement, held together only by moderately strong hydrogen bonds with O···O distances > 2.73 Å.[39] The carbonate group was previously suggested to be disordered at room temperature, leading to speculations about a centrosymmetric space group.[40]

A recent investigation[39] at different temperatures has shown that the carbonate group in washing soda is ordered at a low temperature (110 K), and confirmed the non-centrosymmetric space group *Cc*. Though most parts of the structure are centrosymmetric, only the orientations of the CO_3^{2-} molecules and a few H atoms violate this symmetry. This behavior is caused by the fact that 20 H atoms at the polyhedra around Na cannot be hydrogen bonded to the three acceptor O atoms of the carbonate group in an equivalent, centrosymmetric way. The most interesting observation, however, is that the CO_3^{2-} molecule is only partially disordered at higher temperatures (270 and 295 K), still maintaining its low-temperature position by ~ 60 and 45 %, respectively. Besides 2–3 new, additional disordered positions, a centrosymmetric equivalent of the ordered carbonate position is occupied by only 10–15%. Thus, the space group *Cc* remains unchanged at all temperatures and no phase transition is observed. The evolution from the ordered structure at low temperatures to a partially disordered system at room temperature seems to be continuous, ending up only 10 K higher at the melting point of soda at 305 K with a complete disorder of the carbonate group and simultaneous break of all connecting hydrogen bonds. This continuous behavior from order to disorder and melting is also reflected in a smooth evolution of optical and spectroscopy data *versus* temperature.[39]

A TETRAGONAL GARNET

Garnets are common rock-forming minerals and have the general formula $X_3Y_2(ZO_4)_3$, space group *Ia*3*d*. In the natural solid solutions of the pyralspite and grandite series, X = Mg, Ca, Fe^{2+}, Mn^{2+}; Y = Al, Fe^{3+}; Z = Si. The structure is built up of a framework of alternating, corner-sharing YO_6 octahedra and ZO_4 tetrahedra, with the X cations in dodecahedrally coordinated positions in-between. In addition to the mentioned abundant elements, even rare elements may form garnet structures, either by synthesis intended for technical applications, *e.g.,* YAG (yttrium-aluminum-garnet), or in nature in special geochemical environments, *e.g.,* Cr^{3+} or Mn^{3+} garnets in chromium or manganese ore deposits. In addition, the silicate tetrahedron can be formally substituted by the larger O_4H_4 tetrahedron to form hydrogarnets, which are mainly found in solid solutions with grossular,[41] and more generally in the grandite series.

The rare mineral henritermierite is an unusual hydro-garnet with the formula $Ca_3Mn_2^{3+}(SiO_4)_2(OH)_4$, space group $I4_1/acd$. The tetragonal symmetry is caused by the special arrangement of the Jahn-Teller elongated octahedra around Mn^{3+}.[42] A detailed view of the structure around the (O_4H_4) tetrahedron is given in Figure 10. In contrast to cubic hydrogrossular,[43] where the next-nearest hydrogen bond acceptors of the OH^- groups are found only beyond 3 Å at the corners of the same hydrogarnet tetrahedron, in henritermierite an elongated oxygen corner of a manganese-bearing octahedron comes close to the (O_4H_4) group and thus forms a moderately strong hydrogen bond (O···O distance ~ 2.76 Å).

Therefore, as expected from the stretching frequency – H bond distance correlation[9] described above, the intense O–H stretching band of henritermierite[42] occurs at considerably lower wavenumbers (~ 3430 cm^{-1}) than that of hydrogrossular[41] (~ 3660 cm^{-1}). Much more interesting, however, is the fact that additional, weaker sidebands at higher frequencies (~ 3510 and 3550 cm^{-1}) are observed (well resolved at 80 K) in henritermierite.

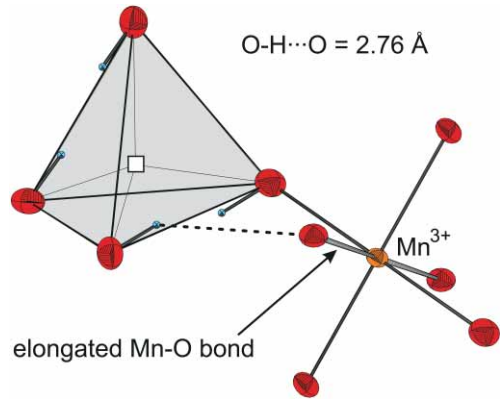

Figure 10. Structural environment of the O_4H_4 tetrahedron in henritermierite.[42]

Since more remote H bond acceptors are only found at the corners of the (O_4H_4) tetrahedron itself, dynamic behavior of the OH^- group hopping or librating between the different H bond acceptors is suggested. This dynamic picture is in better agreement with orientations obtained from polarized spectra and supported by large ADP ellipsoids in neutron refinements of the hydrogarnet group.[42,43]

VERY STRONG HYDROGEN BONDS

Very strong (very short) hydrogen bonds with donor–acceptor distances of 2.40–2.50 Å are found in a number of synthetic compounds and also in rare minerals.[4,11] Their IR spectra are characterized by an extremely wide band at very low wavenumbers around 1000–1500 cm^{-1}, which resembles an increasing, wavy background line, interfering mostly with sharp bands of other structural units.[7] The reason for this peculiar behavior is the enormous anharmonicity of the stretching vibration, operating in an asymmetric double-well potential, and resulting in resonance phenomena such as transmission windows and combinations with low-energy modes of the whole H bond.[10–13] On the other hand, H bonds with the shortest natural bond lengths (~ 2.40 Å) are considered to be symmetric, *i.e.*, O–H = 1.20 Å = H···O, which is reflected in decreased anharmonicity caused by a single-minimum potential, and consequently narrower bands.[7] An extremely short, symmetric H bond was observed under high external pressure in the high-pressure phase of ice VII with an O···O distance of ~ 2.20 Å.[44]

In the isostructural minerals pectolite, $NaCa_2[Si_3O_8(OH)]$, and serandite, $NaMn_2[Si_3O_8(OH)]$, space group $P\bar{1}$, the silicate chain (Figure 11) hosts a hydroxyl group, where both donor and acceptor atoms are part of the silicate chain. The O···O distances are 2.45–2.48 Å. The IR spectra acquired with polarized radiation (Figure 12) show a flat background line and the sharp bending mode of the OH^- group at ~ 1400 cm^{-1} perpendicular to the chain direction (***E*** || *c*), and the characteristic O–H stretching band of a very strong H bond parallel to the chain direction (***E*** || *b*).[45] The extremely broad band shape starting at 3500 cm^{-1} and extending down to below 500 cm^{-1} with wavy appearance and transmission windows (gaps at ~ 1200 and 700 cm^{-1}) in the region of the silicate modes (at ~ 1000 cm^{-1}) confirms the strong anharmonicity. Thus an asymmetric double-well potential and the possibility of proton dynamics (proton transfer) between the two minima (one closer to O3, the other closer to O4) is most likely. This spectroscopic evidence for proton transfer was confirmed by a recent accurate single-crystal neutron diffraction study, where a second position of the proton (with a lower site occupancy factor) in this H bond close to O4 could be identified in a contour map and refined.[46]

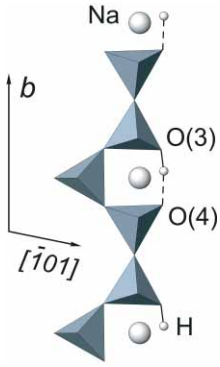

Figure 11. Structural environment of the silicate chain of pectolite and serandite with a very short hydrogen bond between two silicate tetrahedra.[45]

In the mineral mozartite, $CaMn^{3+}O[SiO_3(OH)]$, space group $P2_12_12_1$, a very strong hydrogen bond with an O···O distance of 2.50 (2.48) Å is observed at 300 (100) K.[47] The interesting point is that the proton position is closer to an O atom of the silicate tetrahedron than to that of the distorted octahedron of Mn^{3+}, whereas it is closer to the octahedron in the isostructural mineral vuagnatite, $CaAl(OH)[SiO_4]$, with Al in the octahedral position.[48] IR spectra[47] acquired with polarized radiation show the characteristic, wide O–H stretching band around ~ 1500 cm^{-1} of a very strong H bond and indicate the anharmonic character of an asymmetric double-well potential. The latter was indicated also by the two different proton positions in the two isotypic minerals, though the protons were located at only one site each.

Minerals and synthetic phases of the natrochalcite series, $AMe_2(ZO_4)_2[(H_2O)(OH)]$; A = Na, K, Rb; *Me* = Cu, Co, Ni; Z = S, Se; may contain a very strong hydrogen bond in the central part of a formal $H_3O_2^-$ group, which was considered symmetric, located at a structural site with point symmetry 2/*m*.[49] In the Na–S endmem-

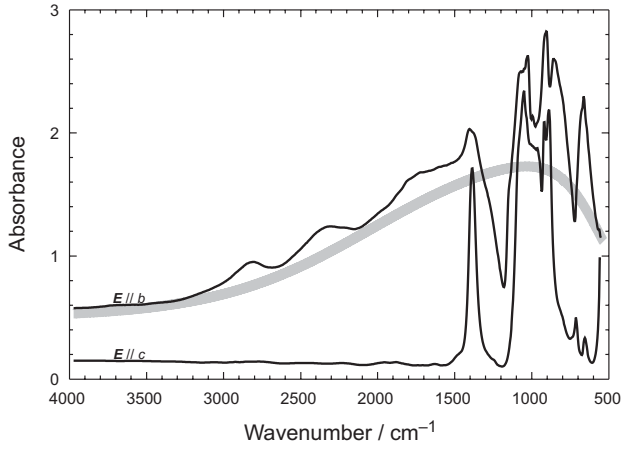

Figure 12. IR absorption spectra acquired with polarized radiation of serandite. The smooth, bold, grey curve indicates the ideal shape of the broad O–H stretching mode in the ***E*** || *b* spectrum of the very strong hydrogen bond.[45]

bers, the O···O distances are as short as 2.44 Å (Cu), 2.43 Å (Co), and 2.42 Å (Ni). Even in these extreme cases, the characteristic band shape and its low-energy position in IR spectra[50,51] recorded with polarized radiation confirmed an asymmetric configuration of the hydrous group. Moreover, a recent accurate single-crystal X-ray refinement revealed a split, disordered H position in an electron density map around the center of the $H_3O_2^-$ group,[51] suggesting proton transfer between the two equivalent, closely spaced sites. The $H_3O_2^-$ unit is therefore better described as H_2O plus OH^- group.

CONCLUSION

Whereas diffraction methods are efficient techniques for solving and refining crystal structures on the basis of their general periodicity, *i.e.*, averaged in space and time, spectroscopic methods (though limited to partial aspects of the structure) are site-specific local probes with a high resolution in space and time. Therefore, the combination of diffraction and spectroscopy provides an ideal tool for obtaining information about complicated structural situations such as disorder in space and time (dynamics), and even to classify and pursue phase transitions from dynamic disorder to structural order.

REFERENCES

1. W. Massa, *Crystal Structure Determination*, 2nd ed., Springer, Berlin, 2004.
2. H. Jagodzinski and F. Frey, *International Tables for Crystallography*, Vol. B, Kluwer, Dordrecht, 1993, pp. 392–433.
3. A. Beran and E. Libowitzky (Eds.), *Spectroscopic Methods in Mineralogy*, EMU Notes in Mineralogy, Vol 6, Eötvös University Press, Budapest, 2004.
4. E. Libowitzky and A. Beran, *EMU Notes in Mineralogy* **6** (2004) 227–279.
5. L. J. Bellamy and A. J. Owen, *Spectrochim. Acta* **A25** (1969) 329–333.
6. K. Nakamoto, M. Margoshes, and R. E. Rundle, *J. Am. Chem. Soc.* **77** (1955) 6480–6486.
7. A. Novak, *Struct. Bond.* **18** (1974) 177–216.
8. W. Mikenda, *J. Mol. Struct.* **147** (1986) 1–15.
9. E. Libowitzky, *Mh. Chemie* **130** (1999) 1047–1059.
10. J. Emsley, D. Jones, and J. Lucas, *Rev. Inorg. Chem.* **3** (1981) 105–140.
11. A. Beran and E. Libowitzky, in: K. Wright and R. Catlow (Eds.), *Microscopic Properties and Processes in Minerals*, NATO Science Series, Kluwer, Dordrecht, 1999, pp. 493–508.
12. D. Hadzi and S. Bratos, in: P. Schuster *et al*. (Eds.), *The Hydrogen Bond – Recent Developments in Theory and Experiments*, Vol. 2, North-Holland Publ. Co., Amsterdam, 1976, pp. 565–611.
13. C. Sandorfy, in: P. Schuster *et al*. (Eds.), *The Hydrogen Bond – Recent Developments in Theory and Experiments*, Vol. 2, North-Holland Publ. Co., Amsterdam, 1976, pp. 613–654.
14. V. Szalay, L. Kovács, M. Wöhlecke, and E. Libowitzky, *Chem. Phys. Lett.* **354** (2002) 56–61.
15. K. Beckenkamp and H. D. Lutz, *J. Mol. Struct.* **270** (1992) 393–405.
16. E. Libowitzky and G. R. Rossman, *Phys. Chem. Minerals* **23** (1996) 319–327.
17. G. R. Rossman, Analytical methods to quantify water in NAMs. *Rev. Mineral.* 2006, submitted
18. M. S. Paterson, *Bull. Minéral.* **105** (1982) 20–29.
19. E. Libowitzky and G. R. Rossman, *Am. Mineral.* **82** (1997) 1111–1115.
20. A. Kurka, *IR-spektroskopische Untersuchungen im OH-Streckschwingungsbereich von Vesuvian und Gossular*, MSc thesis, 2002, University of Vienna, Austria.
21. G. A. Lager, X. Qianyen, F. K. Ross, G. R. Rossman, T. Armbruster, F. J. Rotella, and A. J. Schultz, *Can. Mineral.* **37** (1999) 763–768.
22. A. R. Pawley, *Contrib. Mineral. Petrol.* **118** (1994) 99–108.
23. E. Libowitzky and T. Armbruster, *Am. Mineral.* **80** (1995) 1277–1285.
24. E. Libowitzky and G. R. Rossman, *Am. Mineral.* **81** (1996) 1080–1091.
25. H. D. Lutz, *Struct. Bond.* **82** (1995) 85–103.
26. G. A. Lager, E. Libowitzky, and A. J. Schultz, *Proc. IMA* **98** (1998) A99, Abstract.
27. S. G. Kozlova, S. P. Gabuda, T. Armbruster, and E. Libowitzky, *Proc. IUCR* **1996** (1996), Abstract.
28. P. Sondergeld, W. Schranz, A. Tröster, T. Armbruster, G. Giester, A. Kityk, and M. A. Carpenter, *Am. Mineral.* **90** (2005) 448–456.
29. E. Libowitzky and T. Armbruster, *Am. Mineral.* **81** (1996) 9–18.
30. R. J. Hill, G. V. Gibbs, J. R. Craig, F. K. Ross, and J. M. Williams, *Z. Kristallogr.* **146** (1977) 241–259.
31. E. Libowitzky and G. R. Rossman, *Eur. J. Mineral.* **9** (1997) 793–802.
32. D. M. Adams and D. C. Newton, *Tables for Factor Group and Point Group Analysis,* Beckman-RIIC Ltd., Croydon, England, 1970.
33. E. Libowitzky, A. J. Schultz, and D. M. Young, *Z. Kristallogr.* **213** (1998) 659–668.
34. E. Libowitzky, T. Kohler, T. Armbruster, and G. R. Rossman, *Eur. J. Mineral.* **9** (1997) 803–810.
35. B. Hertweck, E. Libowitzky, and G. Giester, *Am. Mineral.* **86** (2001) 1282–1292.
36. B. Hertweck, T. Armbruster, and E. Libowitzky, *Mineral. Petrol.* **75** (2002) 245–259.
37. B. Hertweck and E. Libowitzky, *Eur. J. Mineral.* **14** (2002) 1009–1017.
38. B. Hertweck, E. Libowitzky, and A. J. Schultz, *Z. Kristallogr.* **218** (2003) 403–412.
39. E. Libowitzky and G. Giester, *Mineral. Petrol.* **77** (2003) 177–195.
40. T. Taga, *Acta Cryst.* **B25** (1969) 2656–2658.
41. G. R. Rossman and R. D. Aines, *Am. Mineral.* **76** (1991) 1153–1164.
42. T. Armbruster, T. Kohler, E. Libowitzky, A. Friedrich, R. Miletich, M. Kunz, O. Medenbach, and J. Gutzmer, *Am. Mineral.* **86** (2001) 147–158.
43. G. A. Lager, T. Armbruster, and F. Faber, *Am. Mineral.* **72** (1987) 756–765.

44. A. F. Goncharov, V. V. Struzhkin, M. S. Somayazulu, R. J. Hemley, and H. K. Mao, *Science* **273** (1996) 218–220.
45. V. M. F. Hammer, E. Libowitzky, and G. R. Rossman, *Am. Mineral.* **83** (1998) 569–576.
46. S. D. Jacobsen, J. R. Smyth, R. J. Swope, and R. I. Sheldon, *Am. Mineral.* **85** (2000) 745–752.
47. D. Nyfeler, C. Hoffmann, T. Armbruster, M. Kunz, and E. Libowitzky, *Am. Mineral.* **82** (1997) 841–848.
48. E. McNear, M. G. Vincent, and E. Parthé, *Am. Mineral.* **61** (1976) 831–838.
49. G. Chevrier, G. Giester, and J. Zemann, *Z. Kristallogr.* **206** (1993) 7–14.
50. A. Beran, G. Giester, and E. Libowitzky, *Mineral. Petrol.* **61** (1997) 223–235.
51. R. Krickl and M. Wildner, *Mitt. Österr. Miner. Ges.* **151** (2005) 73, Abstract.

SAŽETAK

Dinamika kristalne rešetke prikazana primjenom difrakcije i spektroskopije

Eugen Libowitzky

Difrakcija je glavna tehnika za određivanje i utočnjavanje kristalne strukture iako daje prostorno i vremenski prosječne podatke o uzorku. S druge strane, spektroskopija je tehnika osjetljiva na položaj strukturnog motiva u kristalu pa je dobra za istraživanje lokalne strukture sa znatnim vremenskim i prostornim razlučivanjem. Kombinacijom obaju tehnika mogu se izvesti dodatni podaci o kristalnoj strukturi, kao npr. neuređenost i dinamika, a isto tako mogu se izbjeći zamke pri određivanju kristalne strukture. U radu su opisana tri minerala, i to lavsonit, hemimorfit i leonit, koji pokazuju faznu pretvorbu iz dinamički neuređene u uređenu strukturu. Postepeni prijelaz iz uređene u dinamički neuređenu strukturu, bez fazne pretvorbe, utvrđen je u sodi za pranje (natronu). Na kraju se daju primjeri protonske dinamike u tetragonskom granatu i mineralima s vrlo jakim vodikovim vezama.